Available online at www.sciencedirect.com
SCIENCE DIRECT®
Journal of volcanology and geothermal research
ELSEVIER
Journal of Volcanology and Geothermal Research 128 (2003) 115–133
www.elsevier.com/locate/jvolgeores

Magnitude scales for very local earthquakes. Application for Deception Island Volcano (Antarctica)

Jens Havskov [a,b], José A. Peña [b], Jesús M. Ibáñez [b,c,*], Lars Ottemöller [a], Carmen Martínez-Arévalo [b]

[a] *Institute of Solid Earth Physics, University of Bergen, Bergen, Norway*
[b] *Instituto Andaluz de Geofísica, Universidad de Granada, Campus de Cartuja s/n, 18071 Granada, Spain*
[c] *Departamento de Física Teórica y del Cosmos, Universidad de Granada, 18071 Granada, Spain*

Received 20 December 2001; accepted 1 October 2002

Abstract

Different magnitude scales are calculated for a set of volcano-tectonic earthquakes recorded in Deception Island Volcano (Antarctica). The data set includes earthquakes recorded during an intense seismic series that occurred in January–February 1999, with hypocentral distances that range between 0.5 and 15 km. This data set is enlarged to include some regional earthquakes with hypocentral distances up to 200 km. The local magnitude scale, M_L, fixed at a hypocentral distance of 17 km, is used as the reference for the other magnitude scales studied in the present work. M_L is determined on a standard Wood–Anderson simulated trace assuming a gain of 2080. Maximum peak-to-peak amplitudes are measured on the vertical components of a short-period sensor. The M_w scale is calculated, in the vertical component, both for P and S waves. The attenuation correction of the ground motion displacement spectra is introduced using data from coda waves studied in the area. The comparison between M_L values and M_w estimations indicates severe discrepancies between both values. A magnitude–duration scale is calibrated from the comparison between coda durations of the recorded events and their assigned local magnitude scales. In order to investigate the causes of the discrepancy between the M_L and M_w values we analyze two possible error sources: a wrong coda Q value, or the effects of the near-surface attenuation that initially are not taken into account in the correction of the ground displacement spectra. The analysis reveals that the main cause of this discrepancy is the effect of the near-surface attenuation. The near-surface attenuation is also the cause of the determination of an anomalous spectral decay slope, after the corner frequency, and the determination of this corner frequency value. This near-surface attenuation, represented by κ, is estimated over the data set, obtaining an average value of 0.025. With this κ value, the M_w scale is recalculated using an automatic algorithm. The new M_w values are more consistent with the M_L values, obtaining a relationship of $M_w = 0.78M_L - 0.02$.

Keywords: Volcano seismicity; Antarctica; magnitude scales; seismic attenuation; near surface attenuation

1. Introduction

The quantification of the size and energy of seismic signals recorded in volcanic environments

* Corresponding author.
E-mail addresses: jens@ifjf.uib.no (J. Havskov), pena@iag.ugr.es (J.A. Peña), ibanez@iag.ugr.es (J.M. Ibáñez), lot@bgs.ac.uk (L. Ottemöller), mamen@iag.ugr.es (C. Martínez-Arévalo).

0377-0273/03/$ – see front matter © 2003 Elsevier B.V. All rights reserved.
doi:10.1016/S0377-0273(03)00250-6

is one of the most important analyses that has to be performed in the study of volcanic seismicity. The identification and location of the sources that produce the different types of volcanic quakes, and the frequency and patterns of occurrence of these events, are also important for monitoring volcanic activity. The evaluation of the amount of energy that a signal contains, and its spatial and temporal variation, is important in order to understand the source mechanism and also to try to predict the probable evolution of the activity. This quantification has to be done using a homogeneous scale, and the best way is the determination of the event magnitude, but this is a difficult task in many cases. Volcanic environments produce several types of seismic signals different from 'normal' earthquakes. In volcanic environments other types of signals related to fluid dynamics, such as volcanic tremors, long-period events or explosions (e.g. Chouet, 1996), are present. The determination of their magnitudes is not always easy, basically because the location of the positions of their sources is not always possible, or because the nature of their wave fields is not well understood. In some cases it is possible to estimate the associated seismic moment for volcanic tremor and long-period events using the reduced displacement (Aki et al., 1977; Fehler, 1983; Gil Cruz and Chouet, 1997; Ibáñez et al., 2000). For volcanic explosions, the procedure is quite different; one possible way is based on the study of the first pulse of the explosion recorded on broad-band stations and involves determining a magnitude scale based on this impulse (Cruz-Atienza et al., 2001).

The determination of magnitudes of volcanic earthquakes (named volcano-tectonic earthquakes) is in many cases difficult. One of the main problems of this study is related to the type of scale used for these studies, its calibration, and the instruments used for the seismic monitoring of volcanic areas: it is not always possible to obtain accurate response curves in many volcanic areas. From the original local magnitude scale M_L developed by Richter (1935, 1958), several magnitude scales have been proposed to determine the size of earthquakes and their associate energy, such as surface-wave magnitude M_s, body-wave magnitude M_b, duration or coda magnitude M_c, or moment magnitude M_w (Lee and Stewart, 1981). All of them are to some degree based on the original M_L scale. M_s and M_b have globally fixed attenuation relations (anelastic attenuation and geometrical spreading), whereas scales used for local earthquakes (M_L, M_c and M_w) usually require a locally determined attenuation relation. In addition, accurate instrumental calibration must be available for the amplitude-based scales. Often, the magnitude scales are exported from one region to another without considering the regional differences. In many cases the differences are small compared to the uncertainty in magnitude determination, but, for volcanic areas, the attenuation might be different enough to seriously bias the obtained magnitude values when using a magnitude scale from a different area. For example, the special structural characteristics of the volcanic environment, such as structural complexity or topographic irregularities, provides a complex attenuation pattern, with very low Q values and/or deviating geometrical spreading values (e.g. Bianco et al., 1999). In this case it is observed that there is no unique Q value for a volcanic environment and it is strongly dependent of the method used (e.g. Martínez-Arévalo et al., 2002). Other factors that make magnitude determination difficult in volcanic areas are the very short epicentral distances, usually shorter than used in tectonic environments. In many cases, the combined effect of geometrical spreading and seismic attenuation is strongly sensitive to a small change in the hypocentral distance, more than in the case of longer distances. Finally, the low magnitude of the recorded events provides a low signal-to-noise ratio that makes their study more difficult. In some cases we can record events with magnitude lower than -2. These difficulties can be solved at the present because we have highly sensitive (16 or 24 bits of resolution) seismic instruments with a good knowledge of their response curve, the signal-to-noise ratio of the recorded earthquakes is quite good, and we are working in areas where the propagation characteristics are well known. Therefore, we can define a specific magnitude scale local to volcanic areas, as, for example,

Del Pezzo and Petrosino (2001) did for Mt. Vesuvio Volcano (Italy).

On the other hand, the determination of the magnitude of events in volcanic environments should be performed in a systematic and rapid way. This is due to the necessity to obtain a fast evaluation of the activity in order to use it as a surveillance element. When the volume of data is reduced, a manual procedure can be applied; however, when the amount of earthquakes is increased, for example with the occurrence of a seismic swarm, the use of automatic algorithms is convenient. These types of automatic algorithms work well when estimating magnitudes in tectonic environments using coda duration, spectral amplitude (M_w) or maximum amplitude (M_L). However, for volcanic seismicity, the automatic procedures can be problematic. For example, the volcanic tremor shows a strong signal, superimposed on the seismic signal, at frequencies below 6 Hz. This tremor introduces bias in the determination of the coda duration, in the determination of the spectral level and in the true peak-to-peak amplitude. Also, the high attenuation observed near the surface of volcanic environments or the expected low magnitude of the volcanic events could be additional sources of bias in the magnitude estimations. The knowledge of instrument response, attenuation of the medium and hypocentral position could allow us to determine directly the energy involved in the rupture process, and therefore the estimation of the magnitude could be a secondary and unnecessary study. However, if we want to compare the size of the earthquakes with recorded events in the past, or with these in other areas, we need to use an absolute reference, and this reference is the magnitude scale. Therefore, the estimation of the magnitude of the earthquakes is still a very useful tool in the study of the seismicity of volcanic regions.

In the present work we anlayzed a set of volcano-tectonic earthquakes recorded in Deception Island Volcano, Antarctica (see Ibáñez et al., 2000, for a description of the seismicity, instruments and volcanic characteristics of the island), belonging to a seismic swarm occurring in January–March 1999 very near the seismic stations (distances less than 5 km), together with a few local and regional tectonic earthquakes occurring in the neighborhood of the island. It is important to point out that the data set analyzed corresponds to volcano-tectonic earthquakes, that is, these earthquakes are based on shear failures, and therefore the models and theories such as those developed by Richter (1935), Brune (1970), Kanamori (1977) or Hanks (1982) can be directly applied. The purpose of this analysis is the determination of their magnitudes using local magnitude, M_L, and moment magnitude M_w (for P and S waves), the calibration of a magnitude–duration scale, M_c, for the volcano and comparison among all scales. The objective is not only to quantify the size of the selected events, but also to study how the different magnitude scales can be applied to volcanic environments and the special considerations that have to be taken into account in order to apply such a scale for the volcanic areas. Also, alternative ways to estimate the magnitude (manually and automatically) of the events will be presented and the relations among them will be discussed.

2. Deception Island Volcano, instruments and data

The volcanic activity of Deception Island Volcano, Antarctica (Fig. 1), has been monitored since 1989 by the Spanish Antarctic Program by different summer surveys (see for example the periodical reports in the Smithsonian reports in http://www.nmnh.si.edu/gvp/volcano/region19/antarct/deceptn/var.htm). This volcano is one of the most active on the Antarctic continent (e.g. Baker, 1990) and its special geodynamic framework, its intense ice–magma interaction and its volcanic risk (the island is the most visited place of Antarctica, with hundreds of visitors every week during the summer months) makes it an important study.

Ibáñez et al. (2000) made a complete study of the seismicity recorded and analyzed at the island in the 1994–1998 period. The results obtained can be summarized in the identification and study of several pure volcanic signals with origins related to water–magma interactions, and the quasi-absence of volcano-tectonic events. However, in Jan-

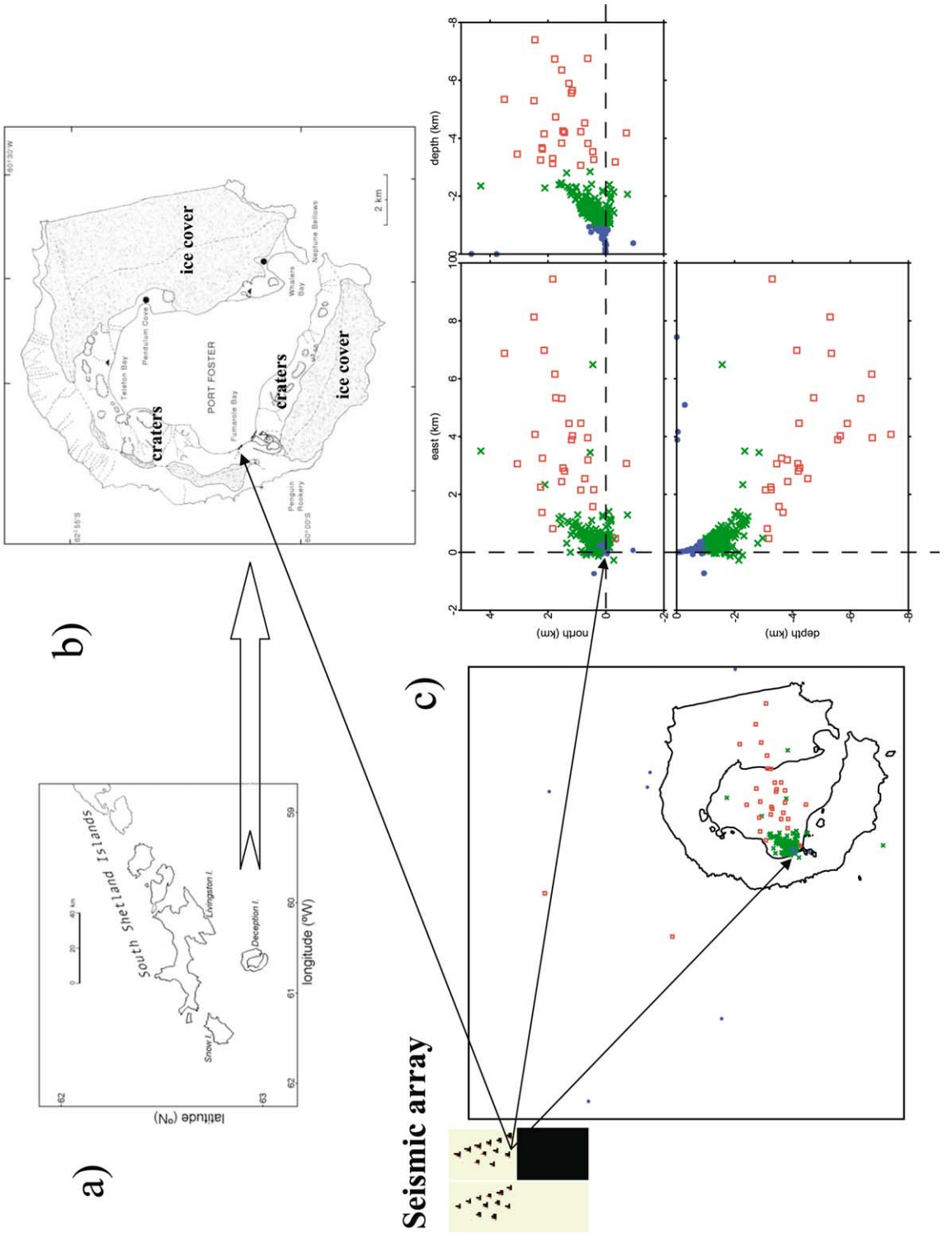
a)
b)
c)
Seismic array
South Shetland Islands
Livingston I.
Deception I.
Snow I.
latitude (°N)
longitude (°W)
ice cover
craters
PORT FOSTER
Pendulum Cove
Teleton Bay
Fumarole Bay
Whalers Bay
Neptune Bellows
Penguin Rookery
2 km
depth (km)
east (km)
north (km)
depth (km)

uary 1999, a radical change in the pattern of seismicity of the island was observed; in the January–March period a seismic swarm occurred composed of more than 3000 recorded volcano-tectonic earthquakes (see Ibáñez et al., 2003, for a description of the volcanic activity of this crisis). Although the magnitudes of the volcano-tectonic events were very small, some of them reached magnitudes M_w larger than 3.4 and were felt by the personnel working on the volcano during this period. Ibáñez et al. (2003) have obtained a preliminary estimation of the moment magnitude of more than 860 earthquakes belonging to this series under the hypothesis of the ω^{-2} decay and using horizontal components. These authors observed values of M_w lower than -1.5 and corner frequencies greater than 30–40 Hz.

The seismic array that recorded the activity was deployed on top of an alluvial fan in close proximity to Fumarole Bay, the most active fumarole system of the island. This array had an aperture of 240 m with stations located along two semicircles, one of radius 120 m and the other of radius 60 m. This array was equipped with three Mark Products L-4 three-component sensors having a natural frequency of 1 Hz, and with seven Mark Products L28 vertical sensors with a natural frequency of 4.5 Hz. Electronic extensions allowed all the sensors to achieve a flat velocity response curve in the 1–50 Hz frequency interval. Recording was performed with two eight-channel, PC-based digital recorders with a dynamic range of 16 bits, recording data at 200 samples/s/channel. Absolute timing at each recorder was achieved via synchronization with the GPS time code (see Saccorotti et al., 2001, for a more detailed description of the instruments and sites).

For the present work we selected a homogeneous subset of the data composed of 153 volcano-tectonic earthquakes uniformly distributed in the whole magnitude range obtained by Ibáñez et al. (2003). To enlarge this interval as much as possible, some local and regional earthquakes to a maximum distance of 200 km were included. We therefore have more than four units of magnitude in the data set for the present study. We did not use volcano-tectonic earthquakes with magnitudes greater than 2.5 because they are saturated in the digital records of the array. The magnitudes of the largest events were previously estimated using a broad-band station placed in Livingston Island (45 km to the north of Deception Island). In Fig. 1 we plot the epicentral distribution of the local and volcano-tectonic events used for the present study. More than 80% of events were located within a hypocentral distance of 5 km, and most of them within 2 km, with focal depths less than 2 km. The errors obtained in the location of the above earthquakes are, on average, ± 0.4 km for hypocentral distances less than 8 km.

3. Local magnitude

In order to calibrate and compare all the magnitude scales used in the present work, we have to use a reference scale. For our study we have chosen the local magnitude scale defined by Richter (1958). The revised scale by Hutton and Boore (1987) for California is given as:

$$M_L = \log A + 1.11 \log \Delta + 0.0019\Delta - 2.09 \quad (1)$$

where A is the maximum peak ground displacement in nm using a filter simulating the low-frequency cutoff of a Wood–Anderson seismometer. Eq. 1 assumes a gain of 2080 measured by the Wood–Anderson seismograph. Δ is the hypocentral distance measured in km. This scale provides a magnitude 3.0 at a distance of 100 km with 1 mm of amplitude on the original Wood–Anderson seismograph. The main difference from the original scale is that the attenuation function

Fig. 1. (a) Map of the South Shetland Island region, Antarctica, showing the position of Deception Island. (b) Map of Deception Island showing the main geological features and some geographical sites. (c) Data selected for this study. Two out of 153 events are outside the map. Symbols of the earthquakes indicate the focal depth of the events: dots, less than 1 km, crosses, between 1 and 3 km and squares, focal depth greater than 3 km. The configuration of the seismic array is represented in the left angle, and its position is represented by the arrows. Note that most events are very close to the array.

has been revised for short distances where only a few data were used to establish the original Richter scale. Hutton and Boore (1987) recommended using a shorter reference distance (fixing the distance at 17 km) if a new attenuation function were to be used for a given region. For example, Del Pezzo and Petrosino (2001) revised the relation for earthquakes belonging to the Vesuvius Volcano (Italy) with the following M_L scale:

$$M_L = \log A + 1.34 \log \Delta - 1.10 \quad (2)$$

We have two possibilities for Deception Island Volcano: (1) to estimate a new M_L relationship including local attenuation values, or (2) to use directly Eq. 1 provided by Hutton and Boore (1987). We have decided to use directly relationship 1 for several reasons:

(a) Eq. 1 includes the attenuation effects in the third term (0.0019Δ). If a new law were estimated for Deception Island this term might be larger than the present one due to the lower Q values observed for the area (e.g. Vila et al., 1995; Martínez-Arévalo et al., 2003). However, due to the very short epicentral distances for the data used, mainly less than 5 km, this attenuation term does not contribute much to the magnitude values. For example, if this term were 10 times greater than for California (which we consider unlikely), the error introduced by using Eq. 1 would be less than 0.1. On the other hand, Q can be considered as the sum of the contribution of scattering and intrinsic attenuation. If, in our region, the scattering effect were more important than for California, we could have a stronger decrease of the peak-to-peak amplitude than expected, without any change of the spectral level. However, due to the short epicentral distances used in this present study (mainly less than 5 km) we do not expect that this effect could greatly affect our M_L estimations using Eq. 1.

(b) The first term of Eq. 1 is mainly related to geometrical spreading, which for California was assumed close to $1/R$. We have no evidence that this value should be modified for Deception Island.

If more data at a varied distance range were available it might be possible to determine a new M_L relationship. However, a new attenuation function would also require us to use a reference distance of 17 km. Therefore only for distances less than 17 km might there be a small magnitude difference compared to using the original relation.

Therefore Eq. 1 has been used to estimate M_L for our selected data. M_L was determined on a standard Wood–Anderson simulated trace assuming a gain of 2080. Maximum peak-to-peak amplitudes (see Fig. 2) were measured on the vertical components of a Mark L4C sensor used as a reference station, the amplitude being determined as half the peak-to-peak amplitude. The simulated Wood–Anderson traces were low-pass-filtered at 30 Hz. The new M_L values show that the reported magnitudes range between −1.5 and 3.0, more than four units.

4. Moment magnitude

The moment-magnitude scale was defined by Kanamori (1977) as:

$$M_w = 2/3 \log M_o - 6.06 \quad (3)$$

where the moment is measured in N m.

In this expression M_o corresponds to the seismic moment that can be expressed, following Brune (1970), as:

$$M_o = (\Omega_o / \Psi_{\theta\phi}\ (4\pi\rho v_s^3 R) \quad (4)$$

where Ω_o is the attenuation-corrected spectral level estimated in the region in which the displacement spectrum remains flat, $\Psi_{\theta\phi}$ is a function accounting for the body-wave radiation pattern and the effect of the free surface (that can be assumed as 0.85), R is the hypocentral distance, v_s is the S-wave velocity and ρ is the Earth density.

To estimate Ω_o and f_o we can use P and S waves, but it is more correct to use only the S-wave displacement spectra. The original Brune spectrum assumed SH waves and therefore we should use horizontal components for these estimations, as Ibáñez et al. (2003) have done for the preliminary estimation of the M_w of the Deception Island data. However, for the present study we have chosen to use the vertical components because:

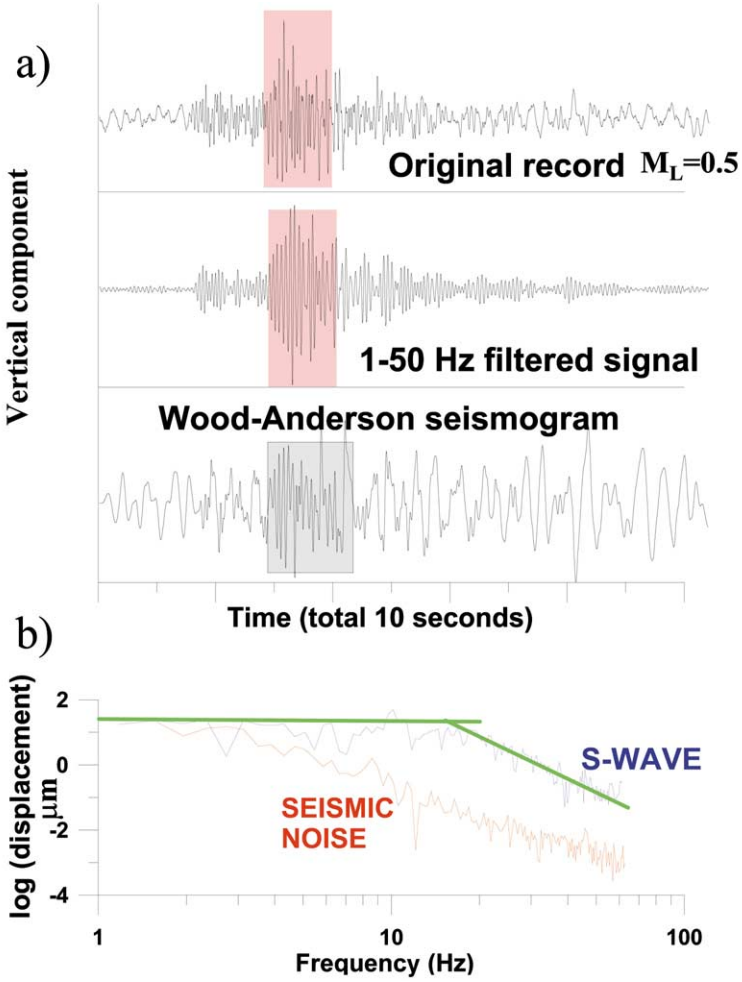

Fig. 2. An example of the data analysis procedure for the M_L and M_w estimations. The earthquake selected has a magnitude $M_L = 0.5$. (a) Original record, bandpass-filtered signal and the corresponding Wood–Anderson seismogram of the vertical component. Gray window over seismogram marks the interval used in the spectral analysis. (b) Spectra of the signal selected in the gray window and the pre-event seismic noise. Straight lines represent the manual procedure used in the estimation of M_w.

(a) On solid rock, experimental studies show that for S or Lg waves, on average there is little difference among amplitudes measured on horizontal and vertical components. However, in volcanic environments, near-surface amplifications are common, which mainly affect the horizontal components (e.g. Bianco et al., 1999). Because the seismic array was deployed on an alluvial fan there was clear site amplification in our data (a factor of 1.5–2 as observed directly on the three-component data) that produces overestimations in the M_w and M_L values. This overestimation is 0.3 units on average.

(b) One of the purposes of the present work is the comparison of the M_w value obtained by using both P and S waves. Because P waves can be better studied in the vertical component, and because the analyzed seismicity has incidence angles close to 45° and SV waves can be observed clearly in the vertical component, we prefer to use vertical displacement for both types of waves.

(c) The seismic instrumentation deployed for

the surveillance of active volcanoes is composed of several types of seismometers, including three-component ones. However, at many volcanoes, the only seismic instrumentation available is composed of vertical sensors. We want to demonstrate that it is possible to estimate these magnitude scales using only this vertical component.

The attenuation-corrected spectra are obtained by applying the Q factor over the ground displacement spectra. The Q factor corresponds to the quality factor of the medium, which is directly related to the seismic attenuation of the region between source and receiver. This Q factor should correspond to the Q value observed for the waves analyzed, in this case the direct P or S waves. If not available, the Q_c factor of the coda waves should be used to correct the spectra. On Deception Island, only a few attenuation studies have been done using coda or other types of seismic waves. Vila et al. (1995) obtained the first Q_c values for the island using relatively long lapse times (they did not consider any lapse time variation and applied the technique over the whole coda). Recently, Martínez-Arévalo et al. (2003) have been working on the determination of the seismic attenuation of the island using different types of seismic waves. These authors have obtained the direct S-wave attenuation using the coda-normalization method (Aki, 1982) for an interval distance between 0.5 and 5 km. The strong influence of the background seismic noise and volcanic tremor did not permit the estimation of any values at frequencies lower than 11 Hz. In the 11–30 Hz frequency band, anomalous behavior of the attenuation values was observed: a decreased Q value between 11 and 21 Hz and an increased Q value after 21 Hz. Therefore it is difficult to apply these values to the S-wave spectra. However, we tested the possibility of applying these direct S-wave Q values to a subset of our data in order to observe the difficulty of application of these results for moment estimation. Due to the variety of results obtained on Deception Island we decided to estimate Q_c with the same set of data used for the magnitude estimation and using the same reference seismic station. Data have been processed using the SEISAN program (Havskov and Ottemöller, 1999) and the single-backscattering model (Aki and Chouet, 1975). Q_c was estimated fixing the start time at 4 s after the origin time with a window length of 5 s, eliminating those estimations in which the signal-to-noise ratio, at the end of the coda, was lower than 3. We assume that the geometrical spreading factor for the coda waves is 1 and the cutoff correlation coefficient in the analysis was fixed at 0.4. The frequency bands used for the analysis were centered at 6, 8, 12, 16 and 32 Hz with a filter width of two octaves. We limited the analysis to frequencies greater than 6 Hz because at Deception Island the background seismic noise (volcanic tremor and oceanic noise) is very high below 6 Hz. The coda envelope was calculated in a sliding window of 5 cycles length and advancing one sample at a time. In this case we obtained a Q_c value of:

$$Q_c = 58f^{0.40} \tag{5}$$

Martínez-Arévalo et al. (2003), using a similar coda length but other frequency bands, obtained a value of:

$$Q_c = 25f^{0.70} \tag{6}$$

Both values are very similar in the 10–20 Hz band, where the seismic moment is determined.

For the P-wave seismic attenuation, we have the results obtained by Martínez-Arévalo et al. (2002) in the analysis of the broadening of the first P-wave pulse for a set of data with hypocentral distance between 0.5 and 8.5 km. They obtained a Q_p value, independent of frequency, of 35 ± 13. However, it is common to use for the determination of the P-wave magnitude a similar attenuation value for P and S waves.

Other parameters used for the estimation of M_o are the density and body-wave velocity. We assumed an average density value of 2.7 g/cm^3. The knowledge of the upper structure of Deception Island Volcano is still under investigation. Previous works of Ibáñez et al. (1997, 2000, 2003) and Saccorotti et al. (2001) have used the results of Grad et al. (1992, 1993) to determine a possible velocity structure of the area for body waves. This model is strongly dependent on the depth and, for example, the average P-wave velocity for the two first kilometers (where the max-

imum concentration of earthquakes has been found) is 1.7 km/s and for S-wave velocity is 1.1 km/s. If we average for the first five kilometers the average v_p is 3.7 km/s and the average v_s is 2.25 km/s. We used P and S velocities of 1.7 and 1.1 km/s, respectively, since this corresponds to the depths of most earthquakes.

4.1. S-wave moment magnitude

The S-wave spectra were determined using the SEISAN package (Havskov and Ottemöller, 1999). We use for ground motion displacement a window starting at the S-wave onset provided by the location procedure established by Ibáñez et al. (2003) and 1 s long. This short window duration is conditioned by the small size of the analyzed data set. The most energetic arrivals of the seismograms are contained in the window and we did not observe significant differences in the results (second order) if a slightly different window is used. The flat level of the spectrum, the corner frequency and the frequency decay were fixed by eye using two straight lines (as plotted in Fig. 2b). For the frequency decay we did not restrict this decay to any specific value.

In Fig. 3a we compare the M_L and M_w values obtained with our data. As observed, there is a nearly linear relationship between M_L and M_w, but the M_w scale provides systematically lower values than M_L for the whole magnitude interval. The experimental relationship between M_L and M_w is:

$$M_L = 1.36M_w + 0.42 \quad (7)$$

Considering that both peak ground displacement and S-wave ground displacement spectrum were measured in the same portion of the seismogram and using the same seismic station, we should expect a linear relationship among M_L and M_w. As Kanamori and Anderson (1975) have shown, M_L must be linearly proportional to log M_o and therefore to M_w, so the following relationship is to be expected:

$$M_L \sim 1.36M_w + 0.42 \quad (8)$$

In our study the relation between M_L and M_w has a slope of 1.36, close to the theoretically ex-

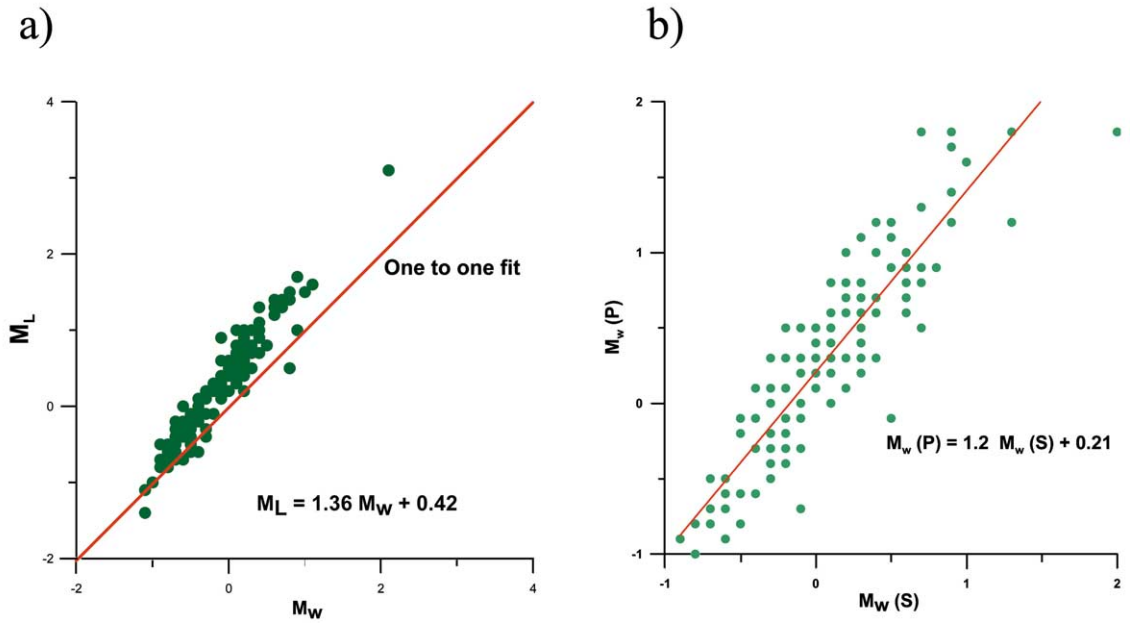

Fig. 3. (a) Relationship between M_L and M_w for S waves. The straight line represents the one-to-one relation. (b) Comparison between M_w for P and S waves. The straight line represents the best fit.

pected value. We also observe that, at least for the small earthquakes of this study, we cannot expect a one-to-one relationship between M_L and M_w.

4.2. P-wave moment magnitude

The P-wave spectra were calculated in a shorter window length than that used for S waves. The average S–P time, measured by Ibáñez et al. (2003), for the data set is 0.7 s, and it is due to the short epicentral distances. To avoid contamination between P and S waves we used a window length of 0.6 s, and we used Q_c as factor of attenuation correction. In Fig. 3b we compare our results with the M_L and M_w for S waves. The experimental relationship between M_w using both P and S waves is:

$$M_w(P) = 1.2M_w(S) + 0.21 \quad (9)$$

As observed, there is a strong relationship between both magnitude estimations, even if they have been determined using different seismic waves but the same attenuation correction.

5. Coda duration magnitude scale

The observations performed by Bisztricsany (1958, 1959), Aki (1969) and Aki and Chouet (1975) indicate that the duration of the seismograms, for local earthquakes, is independent of the nature of the seismic source, epicentral distance or regional geology, but strongly dependent on the magnitude of the seismic events. In this case it is possible to define a new magnitude scale that could relate the duration of the seismograms and the magnitude, the so-called magnitude–duration scale. Therefore, it is possible to calibrate a magnitude–duration scale for Deception Island Volcano measuring the seismogram duration for the same data set used in the M_L and M_w determinations. Due to the high level of background seismic noise and the presence of volcanic tremor superimposed on the signals at low frequencies, we bandpass-filtered our seismograms in the 10–15 Hz band (Fig. 2). The duration was determined manually over the filtered trace. The M_c scale has been estimated by comparing the duration of every seismogram with the previously assigned M_L value (Fig. 4). This plot shows a wide dispersion of the data and therefore a low correlation coefficient. The obtained law is:

$$M_d = (2.8 \pm 0.3)\log \tau - (2.7 \pm 0.3) \quad (10)$$

where τ is the seismogram duration. The correlation coefficient is $\rho = 0.7$. It is important to indicate that this law is limited for the magnitude interval between -1 and 3 where M_L was estimated. Due to the short distances, no distance correction was used.

The dispersion of the data can be attributed to both the errors in the determination of the signal duration and in the different noise levels present in our data. The level of noise present at Deception Island Volcano is dependent on the severe meteorological conditions that change suddenly with winds faster than 100 km/h, rain, marine waves, tides and the volcanic tremors. This means that changes in the level of seismic noise introduce a strong dispersion in the data. For example, for earthquakes of $M_L = -0.5$, the measured durations range between 6 and 10 s, and for earthquakes of magnitude $M_L = 1$, between 10 and 18 s.

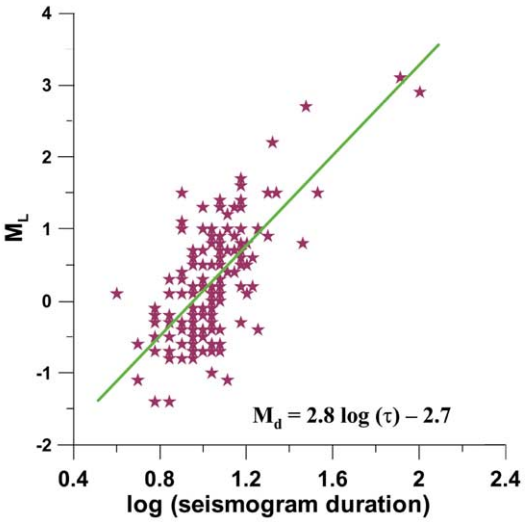

Fig. 4. Relationships between M_L and coda duration. The straight line represents the obtained fit for the magnitude duration scale.

6. Discussion

6.1. Attenuation effects

In the comparison between M_w and M_L for S waves (Fig. 3) we observed that M_w was systematically lower than M_L for the whole magnitude interval. A possible explanation for this difference could be an incorrect attenuation correction for M_w. A possible explanation is: we have used a too high Q value that did not take into account all the contributions of the real attenuation of the zone. Observing our results we can distinguish several indicators that imply that attenuation should be re-calculated:

(1) The observed spectral decay is very rapid after the corner frequency. The obtained average slope in the log–log ground displacement spectra is −3.6, whereas the expected value is −2.0 for the Brune model. In Fig. 5a we plot this spectral decay against magnitude, observing that there is no relation between them. As observed, the spectral decays show values larger than −2, in some cases reaching up to −7.

(2) The relation between M_L, corner frequency and stress drop shows anomalous behavior. In Fig. 5 we show both relationships. It can be observed that f_o tends to increase when magnitude decreases, but clearly stress drop increases when magnitude increases. This variation of the stress drop with magnitude is not consistent with the self-similarity theory. We should expect a more or less constant stress drop for our magnitude range.

(3) The corner frequency values obtained at low M_L estimations are very low. For example, earthquakes with magnitude $M_L = 0$ have been observed with an average corner frequency of 20 Hz. For a stress drop of 5 bar, Lee and Stewart (1981) reported the following relationship:

$$\log f_o = 2.1 - 0.5 M_L \quad (11)$$

In this case we should thus expect a theoretical corner frequency of 126 Hz. In case of lower stress drops the f_o value must be lower than 126 Hz, but not as low as 20 Hz as observed in our data.

Therefore, we could assume that the high-frequency energy of our data has been lost and some strong attenuation must be present. This strong seismic attenuation can be interpreted in two possible ways: (a) the Q_c value used must be lower for the region, or (b) there is a strong near-surface attenuation. Let us study both possibilities.

(a) **A wrong coda Q value**. If the true Q_c value is lower, those earthquakes located far from the seis-

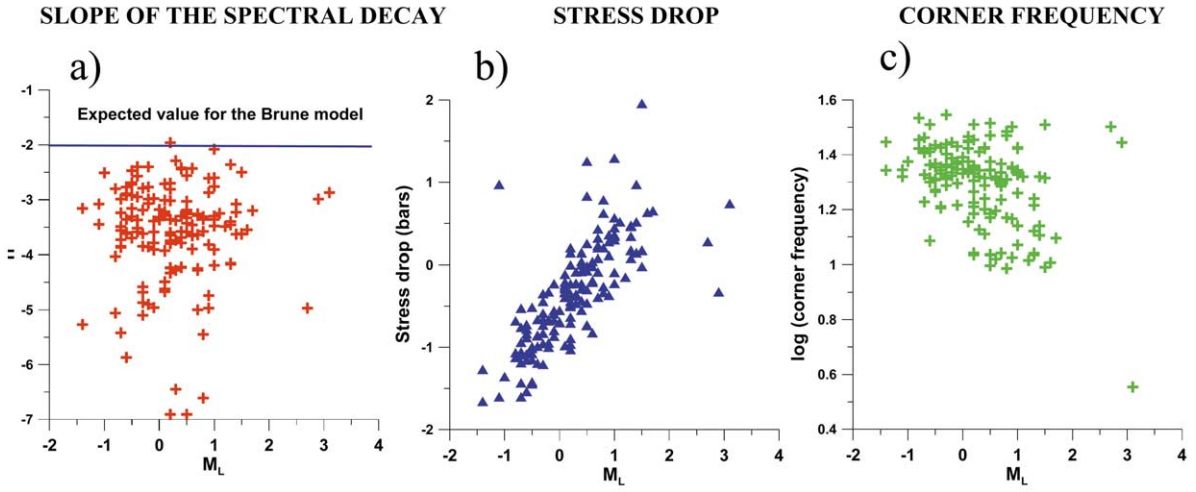

Fig. 5. Slope of the spectral decay versus M_L (a), stress drop versus M_L (b), and corner frequency versus M_L (c). The straight line shows the expected slope decay for the Brune model.

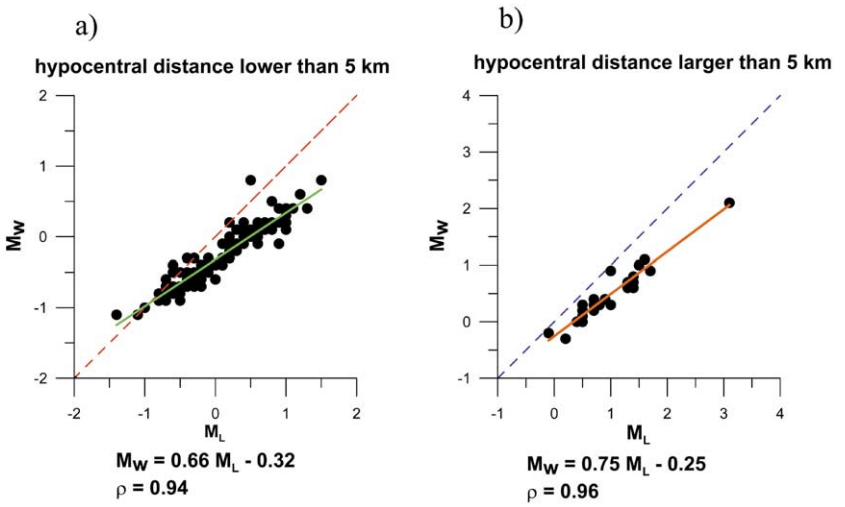

Fig. 6. M_L as a function of M_w. Panel a shows events at short hypocentral distance (< 5 km) and panel b shows events with hypocentral distance larger than or equal to 5 km. The predicted relationship is represented by the dashed lines; the continuous lines show the real relationship.

mic antenna should be affected more by this bias than nearer events. To test this hypothesis we divided our data set into two subsets according to their hypocentral distances: less than 5 km, and therefore volcano-tectonic earthquakes, and more than 5 km. Then we calculated again the M_L and M_w relationship. If the Q_c value is wrong, then we should expect a different relationship according to the hypocentral distances. Observing Fig. 6, there is only a slight difference between both relationships. This result indicates that the regional Q-correction is adequate for long distances and therefore we are confident that the Q_c value used in our analysis is more or less correct.

(b) **Near-surface attenuation**. In recent years it has been shown that at practically all recording sites, even on solid rocks, the first 1–2 km, below the seismic station, has a very severe seismic attenuation (e.g. Hanks, 1982; Abercrombie, 1995; Hough, 1996). If we assume a constant Q near the surface, we can write the amplitude of the recorded waves as:

$$A(f,t) = A_0 e^{-\pi f \int_{\text{surface}}^{t} dt/Q} = A_0 e^{-\pi f t^*} \quad (12)$$

where $A(f,t)$ is the observed amplitude at the seismic station, A_0 is the amplitude before the effect of the near-surface attenuation and the near-surface attenuation is described by a distance-independent function named t^*. Experimentally the values of t^* commonly range between 0.02 and 0.06 (Anderson and Hough, 1984; Abercrombie, 1997; Margaris and Boore, 1998) and are commonly called κ for studies of local seismicity. The t^* name is used only for teleseismic distances.

One of the effects of this near-surface attenuation is that it severely limits the spectral content at high frequencies. This effect will result in the displacement spectrum showing a lower corner frequency, f_κ, than the true value. This observed corner frequency can be calculated as the frequency that appears when the spectral amplitude is reduced to half, therefore:

$$e^{-\pi \kappa f_\kappa} = 0.5 \quad (13)$$

and thus:

$$f_\kappa = \frac{0.223}{\kappa} \quad (14)$$

In our study we measured corner frequencies predominantly around 25 Hz for the smaller earthquakes. Therefore we should expect a κ value around 0.01. This judgment is subjective because the corner frequency might be read when

the spectral amplitude were reduced to 0.25. In this case we should get a κ value close to 0.02.

However, we have a procedure that permits us to estimate experimentally the κ values. The combined effects of near-surface attenuation and seismic attenuation can be expressed as:

$$A(f,t) = A_0 t^{-1} e^{-\pi f \kappa} e^{-\pi f t/Q(f)} \quad (15)$$

Observing the ground displacement spectrum of an earthquake, in the frequency interval in which $f > f_0$ we should expect that this segment, in a double-logarithmic space, is a straight line with a slope of $-\pi(\kappa + t/Q)$, with the assumption of a frequency-independent Q. If the t/Q value is small, the observed slope will be directly proportional to κ and this factor could be estimated for short epicentral distances, without knowing the Q value. If $Q(f)$ is known, then the ground displacement spectrum can be first corrected by this value and κ determined directly. This is the well-known spectral decay method.

Now we can show how κ can affect the spectral studies of our data. In Fig. 7 we show a typical

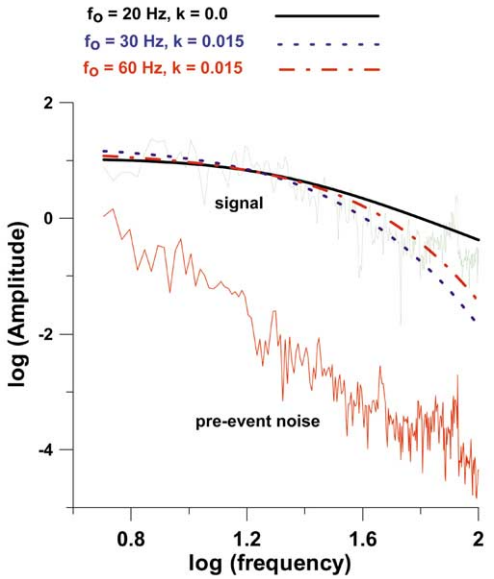

Fig. 7. An example of a Q-corrected spectrum. In the plot, the spectrum of the seismic pre-event noise is represented in order to show the signal-to-noise ratio. The three continuous curves show the theoretical spectrum with different corner frequencies (20, 30 and 60 Hz) for $\kappa = 0.015$.

Q-corrected spectrum of a volcano-tectonic earthquake from the 1998–1999 seismic swarm, with a good signal-to-noise ratio, of $M_L = 0.3$. In the manual procedure used to estimate M_w, we read the corner frequency at 20 Hz and observed a spectral decay greater than $1/\omega^2$. The expected theoretical Brune model, with a spectral decay of $1/\omega^2$, and without taking into account any κ value calculated using the observed parameters, is plotted in Fig. 7 (solid line). This theoretical curve does not fit the experimental data. Now, let us assume a realistic κ value of 0.015. In this case we will need higher f_0 values to fit the theoretical curves to the experimental data. Furthermore, as is also represented in Fig. 7 (dashed line), the theoretical curves obtained using different values of f_0 (between 30 and 60 Hz) are very similar. From this result we can conclude that our experimental data do not allow us the resolution of the true corner frequency value, even in cases with a very good signal-to-noise ratio. Fortunately, for the purpose of our study we do not need to know the true corner frequency value. However, it is very important that the true spectral level is determined with the correct attenuation value, even if it might not be possible to obtain the correct corner frequency value.

Similar tests were done on several other volcano-tectonic earthquakes, indicating that κ could range between 0.010 and 0.030 and is apparently different for different events even with similar short epicentral distances. These discrepancies could be due to many causes, such as different signal-to-noise ratios, or magnitudes, or something else. However, we are interested in determining an average κ value for our data to be useful for the magnitude determination. For that reason we will determine κ using the spectral decay method.

6.2. Experimental determination of κ

A data set of 34 events, with low magnitudes and hence flat source responses up to high frequencies, were collected. All of them have manually observed corner frequencies above 25 Hz, and therefore we are sure the analyses would not be affected by the corner frequency. As dis-

Table 1
Calculation of κ as a function of frequency band

Frequency band (Hz)	κ	S.D.	N
8–20	0.023	0.025	10
8–25	0.027	0.008	11
8–30	0.024	0.007	17
8–35	0.027	0.006	22
8–40	0.031	0.007	22
8–45	0.034	0.007	21
8–50	0.033	0.006	18
8–55	0.035	0.005	14
8–60	0.035	0.004	14
8–65	0.035	0.002	7

S.D. is standard deviation of the average of κ and N is the number of events used.

cussed above, the real corner frequency is probably much higher. The standard method of spectral decay was then used. The spectrum was calculated, corrected for Q as given above, and a straight line fitted to the decay of the spectrum from which κ was calculated for each event and then averaged. The signal-to-noise ratio was checked at every point and required to be at least 2, and a correlation coefficient of 0.5 was needed to include the data in the average. The calculation was done in different frequency bands (see Table 1). Fig. 8 shows all the spectra, for S and P waves and the log average value for both types of waves.

Increasing the frequency band should theoretically not affect κ as long as we are well above the corner frequency. From Table 1 it is seen that κ remains stable until the upper frequency limit is 40 Hz and then slowly starts increasing. This means that the corner frequency of the data used probably is above 40 Hz for all these high-frequency test events. The longer frequency bands also give more stable results. The average κ value derived from Table 1 is 0.031, but, taking into account only frequencies below the probable corner frequency (around 40 Hz), we have an averaged κ value of 0.025.

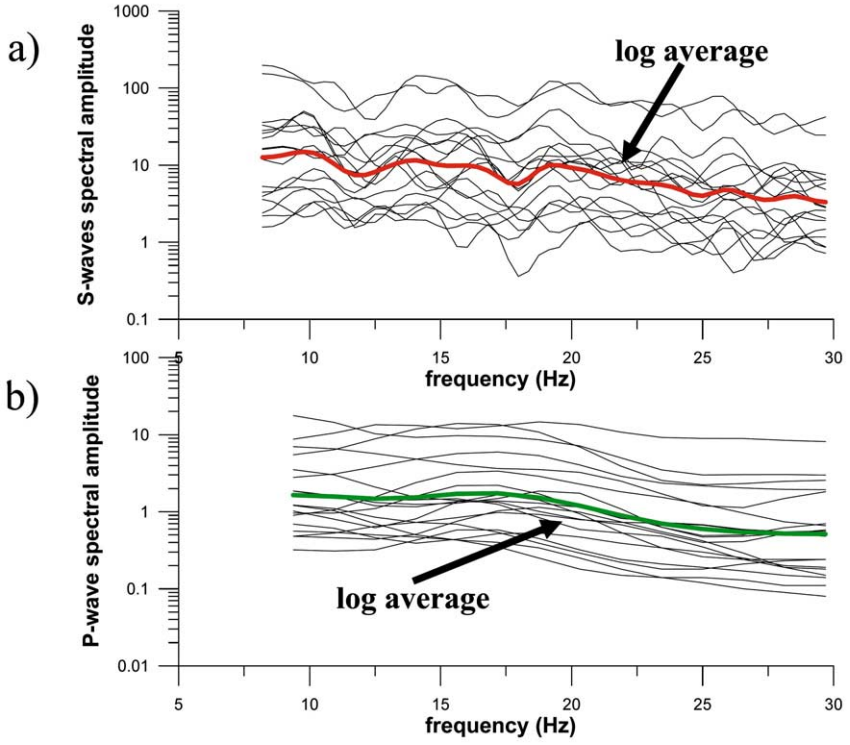

Fig. 8. Procedure for the estimation of κ. (a) The S-wave spectra and the log average spectra (dark line). (b) The same procedure for the P-wave spectra.

6.3. Automatic processing for the magnitude momentum of volcanic earthquakes

Once we know the expected κ value for Deception Island Volcano and the effect of this attenuation on the spectral parameters, it is necessary to re-calculate the M_w estimations taking into account this near-surface attenuation. Due to the large number of data analyzed in the present work, an automatic procedure to estimate the spectral parameters could be convenient. The use of an automatic determination would be very useful for systematic determinations, and especially for volcanic environments in which an accurate and rapid determination is needed. In this study we will check the procedure recently developed by Ottemöller and Havskov (2003). These authors have shown that, even for small earthquakes, like our data set, it is possible to automatically determine the spectral parameters. The idea is to use generic algorithms to fit the experimental data, after correction for seismic attenuation, to the Brune model and to determine automatically the corner frequency and the spectral level. This fast way to estimate the spectral parameters can also be used to check the influence of the different κ values on the magnitude. Before starting the automatic determination we need to check how well this automatic algorithm works with our data set. This test can be done by comparing the M_w values obtained manually in the previous section with the values of the automatic procedure using a κ value equal to 0. This comparison is plotted in Fig. 9a, observing that both manual and automatic M_w determinations are nearly the same, with the trend of the automatic algorithm providing a slightly greater M_w value. The experimental fit between both estimations is:

$$M_{w(auto)} = 1.00 M_{w(manual)} + 0.17 \quad (16)$$

However, there are significant differences between automatic and manual procedures in the determination of the corner frequencies (Fig. 9b). Automatic processing provides corner frequencies systematically lower than the manual determination. This discrepancy can easily be explained as due to the steep decay of the experimental S-wave ground displacement. As

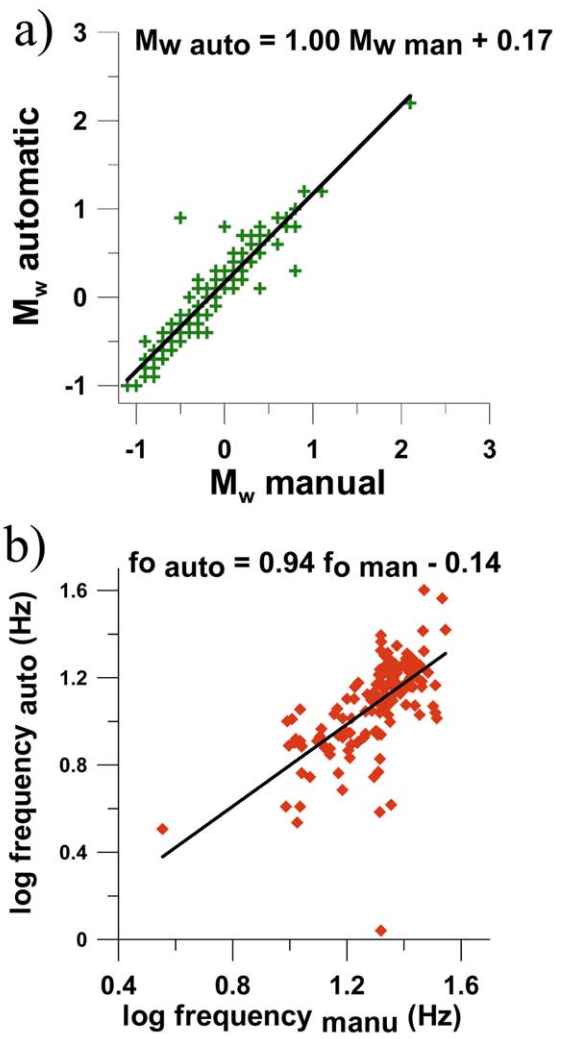

Fig. 9. Comparison between automatic M_w and manual M_w (a) and automatic corner frequency versus manual corner frequency (b).

mentioned previously, the average manual slope was −3.6, whereas the automatic algorithm tries to fit the experimental data to a spectrum of slope −2. This forces the automatic determinations to have lower corner frequency values and it is also the reason for the slightly different M_w estimations. Thus we can say that the automatic procedure works quite well for the M_w estimations for Deception Island Volcano data, although it does not get the observed corner frequency values. Again, because our purpose is the determination

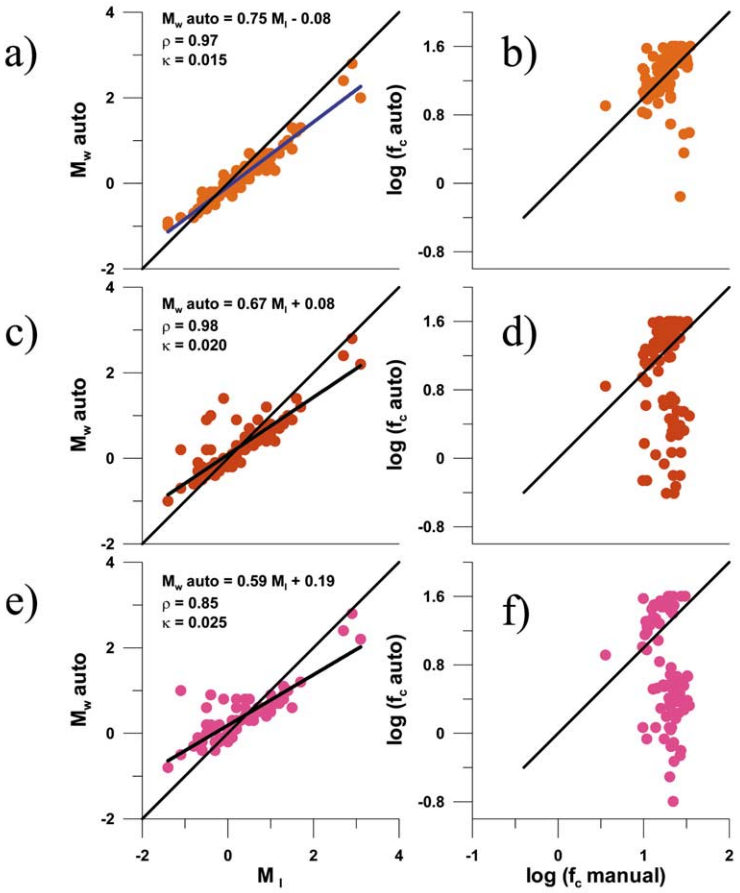

Fig. 10. Comparison between automatic processing using different κ. To the left is shown the automatic M_w vs. manual M_L and to the right automatic corner frequencies vs. manual corner frequencies.

of the magnitude values of our data, and not to obtain source models, we are confident that this automatic procedure is a powerful and fast tool in the study and surveillance of volcanic seismicity.

Finally, we apply this automatic algorithm to our data set to estimate again M_w with different κ values. We compare (Fig. 10) the manual reference M_L values with those M_w values obtained automatically and with different κ values (0.015, 0.020 and 0.025). Also, in Fig. 10 a comparison between manual and automatic corner frequencies is provided. In Table 2 we show the relationship between the M_L values and the derived M_w ones. When κ is changed from 0 to 0.015, we still get a good fit to the data, and average moment magnitudes are increased by 0.27 relative to M_L. We

Table 2
Results of automatic processing

κ	Average M_L	Average M_w	$M_L - M_w$	Number of events
0.000	0.22	−0.15	0.37	148
0.015	0.23	0.13	0.10	128
0.020	0.34	0.31	0.03	105
0.025	0.39	0.42	−0.03	88

also see that the automatic corner frequencies are higher than the manual ones. Further increasing κ makes the corner frequency determination unstable and fewer events are fitted automatically. This is probably caused by trying to push the corner frequency to higher frequencies where the automatic fitting cannot solve them. This is also indicated by the increasing average M_w of the events fitted automatically. From Fig. 10, we see that the highest corner frequencies are about 40 Hz, which is also the limit determined above by the manual determination of κ. We have two possibilities to explain the observations:

(1) If we believe in self-similarity and the ω^{-2} model, the data cannot resolve the corner frequency for most of the events.

(2) Alternatively, we could use a different source model with a steeper decay, like the ω^{-3} model, which would require only a modest change in attenuation and automatic fitting would work well. The real corner frequencies would have to be lower.

Solution (2) seems the less likely since this would not explain the spectral decay below 20 Hz where the ω^{-3} model is also supposed to be flat. We therefore conclude that the data must be corrrected for κ to get a reliable spectral level. However, this will make automatic fitting difficult and 'true' corner frequencies cannot be determined. The automatic determination is a bit more problematic with this data set without changing the standard fitting procedure to only look for the flat level. But then it might not work for larger events. Since the fitting works very well with $\kappa = 0.015$ and the difference in M_w between $\kappa = 0.015$ and $\kappa = 0.025$ is only about 0.1 (also seen from Table 2), the M_w were calculated automatically with $\kappa = 0.015$ and 0.1 magnitude unit was added. For this data set, the relation between M_w and M_L is then:

$$M_w = 0.75 M_L - 0.02 \quad (17)$$

and the two data sets have on average the same magnitude (Table 2). It thus seems that there is a good consistency between the independently determined local and moment magnitudes.

The above discussion can also be done for direct P waves, observing similar effects.

Table 3
The calculated Q_T values combining the effect of Q_c and Q_κ for different values of κ

κ	Q_T	
	10 Hz	20 Hz
0.015	74	85
0.020	64	72
0.025	56	62

6.4. Can we use other Q values?

The inclusion of the κ effect on the attenuation-corrected ground displacement spectra has been due to the fact that Q_c attenuation does not include the effect of near-surface attenuation. Now we could ask if other Q values, containing the total effect of Q, could be used for the M_w estimations instead of Q_c. Martínez-Arévalo et al. (2003) have calculated the Q value for S waves using different techniques for the same data set. One of them has been the broadening of the P and S-wave first pulse, obtaining a value of Q_β independent of the frequency between 48 and 68 as a function of the constant used. From the κ value we can derive a Q value assuming an average travel time for our seismic waves. As reported in a previous section, we consider an average S wave of 1.1 km/s and an average hypocentral distance of 2.5 km, therefore the estimated travel time is around 2.3 s. As reported, the κ values for our area could be 0.015, 0.020 or 0.025, equivalent to Q_κ values of 151, 114 and 91, respectively. In our frequency interval of interest, 10–20 Hz, Q_c ranges between 146 and 192. The combined effect of Q_c and Q_κ provides a total Q_T that could be estimated as:

$$Q_T^{-1} = Q_c^{-1} + Q_\kappa^{-1} \quad (18)$$

In Table 3 we give the calculated Q_T values combining both effects.

The combined effect of both attenuation parameters is very close to the Q value derived using the broadening of the first pulse method. Therefore, in this case, it could have been possible to use only the Q_β from the broadening of the S-wave pulse method to obtain correct ground displacement spectra. Martínez-Arévalo et al.

(2003) also derived Q_β using the coda normalization method, but they obtained values close to or larger than Q_c. The reason is that Q_c or Q_β using the coda normalization method does not include the near-surface attenuation.

7. Conclusions

In the present work we have calculated the magnitude of a set of volcano-tectonic earthquakes recorded in Deception Island Volcano (Antarctica). We have shown that it is possible to calculate the local magnitude value (M_L) of these very local events using the standard local magnitude relation and using the vertical component of the ground displacement. The determination of the moment magnitude scale (M_w) has shown that the correction of the ground displacement spectra using Q_c attenuation values seems to work correctly for regional distances, but provides systematic differences with the M_L estimations for very short epicentral distances. These discrepancies can be interpreted in terms of a near-surface attenuation effect that is not taken into account in the Q_c estimations. This effect can be accounted for by focusing the κ factor (t^*) that has to be included in the correction of the ground displacement spectra. Once this κ value is considered, a good fit between M_L and M_w for very local earthquakes is obtained. One important result observed in the present work is that it is possible to estimate M_w using P waves instead of S waves. This result opens a new way to estimate the magnitude of very local earthquakes when the recorded S waves are saturated. Finally, we want to point out that the automatic algorithms to calculate magnitude, based on generic algorithms, work correctly in those kinds of environments, and therefore could be a fast and powerful tool in the routine procedure to mitigate the hazard inherent in volcanic environments.

Acknowledgements

We gratefully acknowledge the very useful comments, suggestions and help of Prof. Edoardo Del Pezzo and two anonymous reviewers. This research has been partially supported by the projects ANT98-1111, REN2000-2908-E, REN2000-2897-E, REN2001-3833 and by the Grupo de Investigación en Geofísica de la J.A. RNM104. We would like to thank the Spanish Army and Navy for providing us with logistical help during the Antarctic surveys in the 'Gabriel de Castilla' base.

References

Abercrombie, R.E., 1995. Earthquake source scaling relationships from −1 to 5 M_L using seismograms recorded at 2.5-km depth. J. Geophys. Res. 100, 24015–24036.

Abercrombie, R.E., 1997. Near-surface attenuation and site effects from comparison of surface and deep borehole recordings. Bull. Seismol. Soc. Am. 87, 731–744.

Aki, K., 1969. Analysis of the seismic coda of local earthquakes as scattered waves. J. Geophys. Res. 74, 615–628.

Aki, K., 1982. Scattering and attenuation. Bull. Seismol. Soc. Am. 72, S319–S330.

Aki, K., Chouet, B.A., 1975. Origin of coda waves: source, attenuation and scattering effects. J. Geophys. Res. 80, 3322–3342.

Aki, K., Fehler, M., Das, S., 1977. Souce mechanism of volcanic tremor: fluid-driven crack models and their application to the 1963 Kilauea eruption. J. Volcanol. Geotherm. Res. 2, 259–287.

Anderson, J.G., Hough, S., 1984. A model for the shape of the Fourier amplitude spectrum of acceleration at high frequencies. Bull. Seismol. Soc. Am. 74, 1969–1994.

Baker, P., 1990. Deception Island. In: LeMasurier, W., Thomson, J. (Eds.), Volcanoes of the Antarctic Plate and Southern Oceans. Antarctic Research Series 48. AGU, Washington, DC, pp. 316–321.

Bianco, F., Castellano, M., Del Pezzo, E., Ibanez, J.M., 1999. Attenuation of short-period seismic waves at Mt Vesuvius, Italy. Geophys. J. Int. 138, 67–76.

Bisztricsany, E., 1958. A new method for the determination of the magnitude of earthquakes. Geofiz. Köl. 7, 2.

Bisztricsany, E., 1959. On a new method of determining earthquake magnitudes. UGGI Série A, Travaux Sci., Fasc. 20, 9–15.

Brune, J.N., 1970. Tectonic stress and the spectra of seismic shear waves from earthquakes. J. Geophys. Res. 75, 4997–5009.

Chouet, B., 1996. Long-period volcano seismicity: its source and use in eruption forecasting. Nature 380, 309–316.

Cruz-Atienza, V.M., Pacheco, J.F., Singh, S.K., Shapiro, N.M., Valdéz, C., Iglesias-Mendoza, A., 2001. Size of Popocatepetl volcano explosions (1997-2001) from waveform inversion. Geophys. Res. Lett. 28, 4027–4030.

Del Pezzo, E., Petrosino, S., 2001. A local-magnitude scale for

Mt. Vesuvius from synthetic Wood-Anderson seismograms. J. Seismol. 5, 207–215.

Fehler, M., 1983. Observations of volcanic tremor at Mount St. Helens volcano. J. Geophys. Res. 88, 3476–3484.

Gil Cruz, F., Chouet, B.A., 1997. Long-period events, the most characteristic seismicity accompanying the emplacement and extrusion of a lava dome in Galeras volcano, Colombia, in 1991. J. Volcanol. Geotherm. Res. 77, 121–158.

Grad, M., Guterch, A., Sroda, P., 1992. Upper crustal structure of Deception Island area, Bransfield Strait, West Antarctica. Antarct. Sci. 4, 469–476.

Grad, M., Guterch, A., Janik, T., 1993. Seismic structure of the lithosphere across the zone of subducted Drake plate under the Antarctic plate, West Antarctica. Geophys. J. Int. 115, 586–600.

Hanks, T.C., 1982. f_{max}. Bull. Seism. Soc. Am. 72, 1867–1879.

Havskov, J., Ottemöller, L., 1999. The SEISAN, earthquake analysis software for Windows, Sun and Linux. Manual and software. Institute of Solid Earth Physics, University of Bergen.

Hough, S.E., 1996. Observational constraints on earthquake source scaling: understanding the limits in resolution. Tectonophysics 261, 83–95.

Hutton, L.K., Boore, D.M., 1987. The M_L scale in Southern California. Bull. Seism. Soc. Am. 77, 2074–2094.

Ibáñez, J.M., Morales, J., Alguacil, G., Almendros, J., Ortiz, R., Del Pezzo, E., 1997. Intermediate-focus earthquakes under South Shetland Islands (Antarctica). Geophys. Res. Lett. 24, 531–534.

Ibáñez, J.M., Del Pezzo, E., Almendros, J., La Rocca, M., Alguacil, G., Ortíz, R., García, A., 2000. Seismovolcanic signals at Deception Island volcano, Antarctica: Wave field analysis and source modeling. J. Geophys. Res. 105, 13905–13931.

Ibáñez, J.M., Carmona, E., Almendros, J., Saccorotti, G., Del Pezzo, E., Abril, M., Ortiz, R., 2003. The 1998-1999 seismic series at Deception Island volcano (Antarctica). J. Volcanol. Geotherm. Res., 128, doi 10.1016/S0377-0273(03)00247-6 (this issue).

Kanamori, H., 1977. The energy release in great earthquakes. J. Geophys. Res. 82, 2981–2987.

Kanamori, H., Anderson, D.L., 1975. Theoretical basis of some empirical relations in seismology. Bull. Seismol. Soc. Am. 65, 1073–1095.

Lee, W.H.K., Stewart, S.W., 1981. Principles and Applications of Microearthquake Networks. Academic Press, New York, 293 pp.

Margaris, N., Boore, D.M., 1998. Determination of $\Delta\sigma$ and κ_0 from response spectra of large earthquakes in Greece. Bull. Seismol. Soc. Am. 88, 170–182.

Martínez-Arévalo, C., Bianco, F., Ibáñez, J.M., Del Pezzo, E., 2003. Shallow seismic attenuation and shear wave splitting in the short period range of Deception Island volcano (Antarctica). J. Volcanol. Geotherm. Res., 128, doi 10.1016/S0377-0273(03)00248-8 (this issue).

Ottemöller, L., Havskov, J., 2003. Robust and fast automatic magnitude determination using a genetic algorithm. Bull. Seismol. Soc. Am. 93, 203–214.

Richter, C.F., 1935. An instrumental earthquake magnitude scale. Bull. Seismol. Soc. Am. 25, 1–32.

Richter, C.F., 1958. Elementary Seismology. Freeman, San Francisco, CA.

Saccorotti, G., Almendros, J., Carmona, E., Ibáñez, J.M., Del Pezzo, E., 2001. Slowness anomalies from two dense seismic arrays at Deception Island, Antarctica. Bull. Seismol. Soc. Am. 91, 561–571.

Vila, J., Correig, A.M., Marti, J., 1995. Attenuation and source parameters at Deception Island (South Shetland Islands, Antarctica). Pure Appl. Geophys. 144, 229–250.